Australian Journal of Crop Science AJCS
AJCS 4(9):757-766 (2010) ISSN:1835-2707

Impacts of inflow mean velocity and its concentration on the head velocity and the cross motion of density current using the hydraulic model

Roozbeh Ghazal*, Amir Khosrojerdi

Department of Water Engineering, Islamic Azad University, Science & Research Branch, Tehran, Iran

***Corresponding author: roozbeh.ghazal@gmail.com; am_khosro@yahoo.com**

Abstract

The behavior of density current in reservoirs and coasts is usually believed to be a very complicated phenomenon. The head velocity of density current entering the reservoir and its lengthwise and widthwise motions are affected by inflow discharge and concentration. To study this issue, first, a hydraulic model was built in a laboratory and then, variation of effective factors studied in an experimental survey. A laboratory rectangular flume (8×3×1.5 meters) was built with Plexiglas. A Turbidity current was prepared in a separate tank filled with water and Kaolinite particles and thereafter, applied to the model through a gate (20×3 cm). Finally, the effects of changes in inflow discharge and its concentration on the head velocity and lateral waves going to the sides were measured precisely. The laboratory results indicated that the head velocity increased due to raising the inflow concentration and velocity. The maximum head velocity was recorded at 1 to 1.5 meters from the entrance gate. As result, the head velocity reduction at the adjacent area for the low-concentration inflow was more than the high-concentration tests (respectively 75% and 23% in average). Measurements indicated that deviation angle of the density of current cross motion from the flow direction is also affected by the inflow velocity and its concentration, varies from 41º - 63º. The high-concentration current runs (more than 4%) increased the angle to the maximum range.

Keywords: density current, head velocity, side motion, Laboratory experiments, Velocity and concentration measurements.

Introduction

After being constructed, reservoirs cause specific effects and impacts on river hydraulic regime. Each year, about 15000 million tones of sediments (5700 million cubic meters) carried to the coasts worldwide (Hoogendoorn, 2006). Sedimentary deposition causes an increase in the reservoir dead volume (Fan and Morris, 1992), influences water intake and sediments entrance into the dam power plants (Boillat et al., 1994; De Cesare, 1998) and also heightens flood risk as a result of increase in the level of delta area bed in the upstream of dam. Gravity currents are flows driven by a difference in density between the current and ambient fresh water of reservoir. Respectively, coarse and fine particles are deposited in upstream and downstream of reservoir during the mass transport processes. In order to perceive the body dynamics and front of density current, Middleton built a laboratory flume (Middleton, 1966). Assuming that entrainment controls the behavior of density current, Ellison and Turner concluded that the features of density current layer are functions of average velocity and overall bulk Richardson's number (Ellison and Turner, 1959). Herbert and Colleagues studied the plunge point depth by examining a triangle section flume (Hebbert et al., 1979). Yu et al. (2000) showed that the coarse particles are deposited in delta area and immediately sink into the plunge point. Garcia (1985) reported that after injection of density current into a 5% sloped flume, course particles cannot be suspended and they deposit at the initial stage. Altinakar et al. (1990) set an experiment with slopes between 0 – 5.6% and used quartz powder with 0.014 and 0.032 mm in diagonal. They noticed that the deposition process decreases the head velocity and increases the thickness of current front (Altinakar et al., 1990). Middleton (1966) found out that in small slope hydraulic flume (<2-3 º), the head velocity rate definitely depends on the slope. Head velocity of the dense current has also been analyzed by Keulegan (1957). According to his experience, the amount of equations is not related to the slope (Keulegan, 1957). The later studies showed that as a result of increase in gravity force and tensions between body, head of density current and the space in which the current is flowing (such as low density ambient water) the rate of slope (5 to 90 degree) does not have any significant effect on the head velocity of density current (Britter and Linden, 1980). The body velocity of density current, which depends on the slope, is 30 to 40% more than the head velocity of current (Middleton, 1966; Kneller et al., 1997, 1999). Therefore, head thickness of density current is increased (Hopfinger and Tochon-Danguy, 1977; Britter and Linden, 1980; Simpson, 1997). Velocity in the body of density current may be about 40% more than the mean velocity of density current body (Buckee et al., 2001). The velocity can reach to the peak of 10 m/s (e.g. Mulder et al., 1997a). Thickness and size variation of the density current head causes the suspended particles velocity to be different from head and backflow current. This condition may lead to current strain and backflow weakness. In several experiments, the front area of flow, separated from the density current body and consequently this event created a new front (Parsons et al., 2007). Lowe et al. (2002) stated that by dividing front area of the density current body into three parts, velocity in forward area of the current is monotonous and very close to the head velocity. But in the back

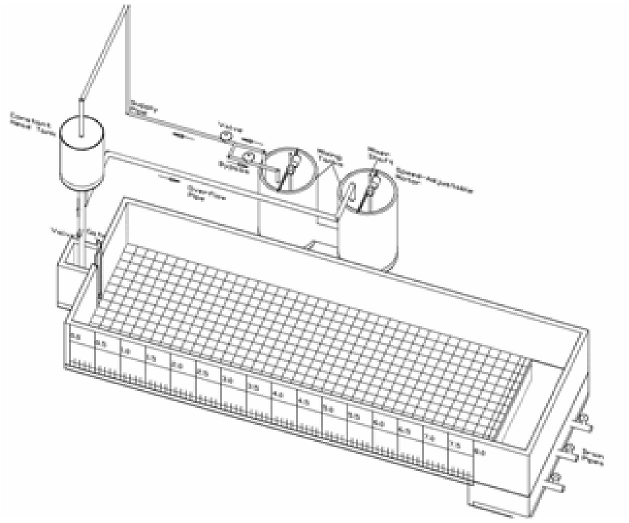

Fig 1. Equipments used for the laboratory modeling

Table 1. Specifications of the sediment used in the experiments

D50 (mm)	D90 (mm)	Density	Settling velocity (mm/sec)	Sediment type
0.01	**0.06**	**2.33**	**0.0636**	Kaolinite

area, the velocity is more turbulent due to lateral movements. It even sometimes does not reach to the front of density current and the velocity rate may vary. Sometimes it even moves with a velocity of 50% more than the head velocity of flow current head. At the rear part of the flow, the current velocity is a bit higher than density current head velocity and is almost monotonous (Lowe et al., 2002). Moghtaderi used Laser-Doppler, isothermal and adiabatic conditions to conclude that the minimum turbulent condition occurs in an area of current where the velocity is maximized and the shear stress is minimized (Moghtaderi, 2004). Following the experiments in a flume (3×0.2×0.6 meter), it was stated that in quantity definition of density current velocity, Froude number plays a crucial role (Marino et al., 2005). This article aims to describe the effects of inflow density current velocity and concentration, upon the longwise and lateral motion of density current head velocity behavior.

Materials and methods

In order to study the behavior of density current, the experiments were performed in a glass-wall tank with 8.5 m length, 3 m width and 1.5 m height. The flume slope was fixed at 2% and the flume bed was covered by ceramic cap (Fig 1). Turbid water containing different percents of various non-cohesive types of Kaolinite was prepared in two separate tanks. The sediment features and specifications have been provided in Table 1. Dense current was transmitted by submersible pump through a pipe to a head tank installed at the upstream of main flume. A head tank with a fixed head was assigned to fix the dense fluid. Afterwards, the water with Kaolin particles entered the flume filled by clear water and the overflow returns to the mixing tanks through the bypass pipe (Fig 2). About 2 m^3 of dense water with prepared in the mixing tanks. Sediment was kept in suspension in the mixing tank by a propeller and the concentration of suspension was maintained by manual addition of water and sediment. The particle concentration of the flow entering the experimental tank was monitored by drawing off samples just above the head tank (Fig 2a). The inflow concentration varied between a minimum of 0.57% to 6%. The gate was rapidly lifted up to provide a steady condition of inflow dense current. Duration of each test was recorded so that by assessing water outflow volume from mixing tanks, we achieved the current discharge by dividing the volume over the time. The inflow discharge took an amount between 28.28 and 175.2 l/s.

Results and discussion

Simulation of natural density current

There are four ways to reach the scale of hydraulic model for the purpose of density current simulation:

1. Building a model with a scale of 1:1
2. Simulation of Froude model
3. Simulation on the basis distorted model
4. Simulation with a non-dimensional model

Modeling density current as well as the ocean coasts conditions with scale 1:1 seems illogical. Therefore scale laboratory modeling is the best practical way to study this phenomenon. Distorted models are used to simulate some density currents conditions. In order to simulate shear stress in bed condition a sharper lengthwise slope is considered for the model (e.g. Postma et al., 1988). Therefore, we should treat the results of the experiment with caution. Also, the Froude model simulates currents' features and behaviors on the basis of a set of non-dimension parameters. Simulation analysis with regard to the type of efficient variable is subdivided into several parts such as Reynolds number, Richardson number and Froude number. Non-dimensional Froude number, Fr, is given by

$$Fr = \frac{V}{\sqrt{g\, h_b \cos\alpha \frac{\rho_f - \rho_a}{\rho_a}}} \qquad (1)$$

In this formula ρf is the inflow density, ρa is the clear water density, h_b the inflow current depth, g the gravity acceleration, α the bed slope and V the inflow mean velocity. The Froude number has been calculated for the prior experiments. The amount greater than 1 is assigned to supercritical conditions (García, 1993; Morris et al., 1998). Underflows monitored in the Katsurozawa Reservoir had densiometric Froude numbers of 0.545-0.876 (Chikita, 1990). The bulk Richardson number (Ri) in density current conditions is as follows

$$Ri = \frac{g(\rho_f - \rho_a)\, h_b \cos\alpha}{V^2 \rho_a} \qquad (2)$$

The Richardson number is usually applied for the diagnosis of the stability of flow (Fukushima et al., 1985; Parker et al., 1986). Richardson number lower than 0.25 refer to the unstable condition of density current. Richardson number smaller than 1 represent supercritical flows regime whereas value larger than 1 represent subcritical flows .Richardson number which is lower than 0.25 shows unstable condition of density current (Simpson, 1987). Richardson's number smaller than 1 represent super-critical flows regime whereas value larger than 1 represent

Fig 2. View of (a) the main flume filled with clear water (b) mixing tank for preparing dense current.

subcritical flow. Also the Reynolds number is calculated using the following formula:

$$Re = \frac{Vh}{\mu} \qquad (3)$$

Where μ is the apparent kinematic viscosity and the Reynolds number delineates laminar (Re<500), transitional (500<Re<2000) and turbulent (Re>2000) flow. Parsons and Garcia demonstrated that the mixing of the ambient fluid and the gravity current's head is dependent on Reynolds number with transition at Re ~2 × 105 (Parsons and Garcia 1998).

Calculating the velocity of density current wave's motions

The density current is affected by drag coefficient in bed and ambient fluid boundaries. Density current in dam reservoir deposits in current forward motion as the particles reduce and with a reduction in velocity. Lee and Yu analyzed their laboratory hydraulic model and concluded that non-dimension mean velocity decreases in lengthwise motions (Lee and Yu 1997). The early experiments and studies show that travelling velocity of turbidity current is almost constant and is estimated through chezy-type equation (Hinze, 1960):

$$U = C\sqrt{g'hS_0} \qquad (4)$$

C takes an amount between 280 and 560 $\frac{cm^{1/2}}{S}$, g´ is the reduced gravity, of density current , S0 is the mean slope of bed and h is the depth of current.
This can also be estimated using the Darcy-Weisbach equation (Harleman, 1961)

$$U = \sqrt{\frac{8}{f(1+\alpha)}}\sqrt{g'hS_0} \qquad (5)$$

This equation remarkably corresponds to field measurements (Lack Mead recorded).In this equation f takes the role of friction factor for the currents in pipes derived from moody diagram. α is a coefficient that only takes the amount of 0.43 and justifies the shear distribution at the interface of density current and ambient water .
Another equation in which α takes zero is also accepted by Mahmood (1987).

$$U = \sqrt{\frac{8}{f}}.\sqrt{g'hS_0} \qquad (6)$$

The friction factor f varies between 0.020 and 0.025.
There are many various theoretical and experimental equations suggested for the density current head velocity, especially in horizontal channels (Simpson & Britter, 1979)

$$U_f = 0.83\sqrt[3]{g'q} \qquad (7)$$

q is the inflow discharge. The non-dimensional velocity of current is calculated through the following equation

$$U_f' = \frac{U_f}{\sqrt{g'h}} \qquad (8)$$

It is estimated to take 0.41 for the horizontal chanel (215×20 cm) and for turbulent and sub critical conditions (Kneller et al., 1997; 1999). In previous researches and presumably in small-scaled models, this amount has been suggested to take 0.44 (Middleton, 1966) and 0.46 (Keulegan, 1958; Barr, 1967).
The following equation is suggested for calculating the head velocity of dense current in low-sloped beds (Bagnold, 1954; Middleton, 1966; Turner, 1979)

$$U_F = 0.75\sqrt{g'h_f} \qquad (9)$$

hf is the head thickness. Lately a coefficient of 0.63 has been suggested instead of 0.75 (Altinakar et al., 1990).The following equation has been developed for a wide range of slopes (Britter and Linden, 1980).

$$\frac{U_F}{\sqrt[3]{g'q}} = 1.5 \pm 0.2 \qquad (10)$$

q is the inflowing unit discharge. The equation has also been approved by numeric method calculations (Chio and Garcia, 1995).
After building a Plexiglas flume (500×30×50 cm), Samothrakis and Cotel (2006) studied the front velocity of density current. The flume slope adjusted to 6 degrees and the length of slope extended to 2 meters. Afterwards the salinity current was fed into the model and subsequently, the head velocity of dense current was estimated to conform with the following equation (Samothrakis and Cotel, 2006).

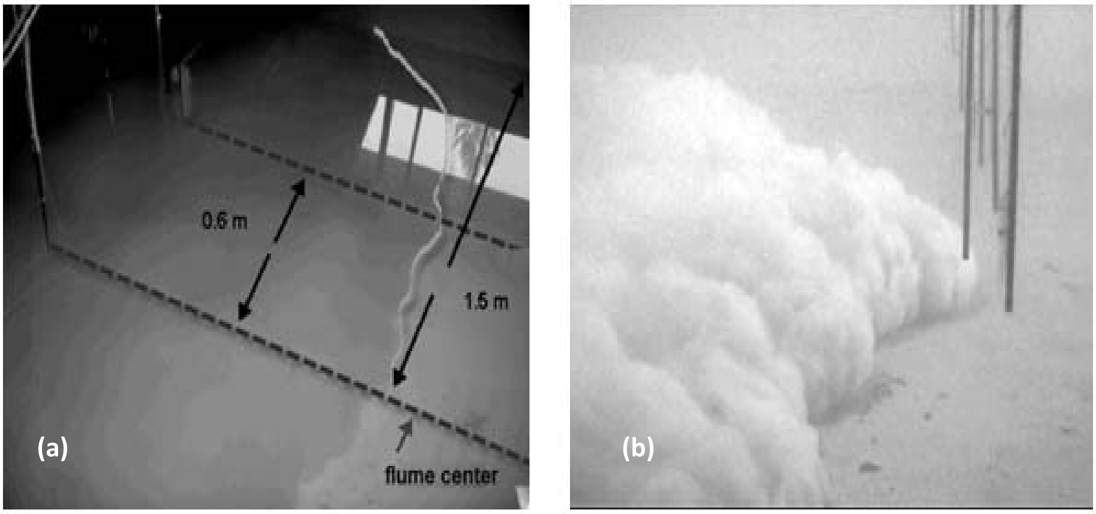

Fig 3. The gravity current front after opening of the gate.

Table 2. Summary of experiments performed

Exp. No.	Description	h_0 (cm)	Q_0 (lit/min)	C_0 (%)	U_0 (cm/s)	g'_0 (cm/s^2)	B_0 (cm^4/s^3)	Ri_0	Re_0	Time (min)
1	Q31C2.1	3	31	2.1	8.50	27.5	14005.2	1.14	2427.39	23
2	Q36C3.1	3	36	3.1	10.00	40.5	24322.7	1.22	2793.34	23
3	Q36C3.55	3	36	3.55	10.00	46.4	27853.4	1.39	2765.11	15
4	Q33C3.92	3	33	3.92	9.17	51.3	28193.4	1.83	2513.35	16
5	Q32C5.1	3	32	5.1	9.00	66.7	36013.3	2.47	2400.55	23
6	Q42C5.54	3	42	5.54	11.67	72.4	50711.6	1.60	3079.26	23
7	Q57C1.65	3	57	1.65	15.83	21.6	20497.8	0.26	4565.81	22
8	Q58C2.06	3	58	2.06	16.00	26.9	25860.5	0.32	4573.18	20
9	Q62C2.93	3	62	2.93	17.17	38.3	39464.3	0.39	4813.51	21
10	Q67C4.56	3	67	4.56	18.50	59.6	66189.2	0.52	4997.70	15
11	Q55C5.13	3	55	5.13	15.33	67.1	61716.9	0.86	4086.91	20
12	Q62C5.42	3	62	5.42	17.33	70.9	73710.9	0.71	4588.10	15
13	Q62C5.58	3	62	5.87	17.17	76.8	79063.2	0.78	4494.90	15
14	Q92C1	3	92	1.0	25.67	13.4	20564.8	0.06	7501.09	15
15	Q93C1.5	3	93	1.5	25.83	19.1	29592.6	0.09	7479.85	15
16	Q99C2.6	3	99	2.6	27.50	33.4	55064.8	0.13	7775.89	15
17	Q74C1.2	3	74	1.2	20.50	15.7	19301.3	0.11	5968.54	15
18	Q123C.57	3	123	0.57	34.17	7.5	15280.2	0.02	10079.94	24
19	Q110C1.19	3	110	1.194	30.67	15.6	28729.1	0.05	8929.68	20
20	Q104C0.8	3	104	0.8	29.00	10.5	18202.8	0.04	8514.72	20
21	Q102C1.3	3	102	1.3	28.33	17.0	28899.6	0.06	8231.72	20
22	Q109C0.6	3	109	0.6	30.33	7.8	14279.8	0.03	8943.44	15
23	Q110C1.04	3	110	1.04	30.67	13.6	25023.6	0.04	8958.79	15
24	Q132C1.3	3	132	1.3	36.67	17.0	37399.4	0.04	10652.81	15
25	Q138C0.65	3	138	0.65	38.33	8.5	19549.7	0.02	11290.39	23
26	Q26C3.27	3	26	3.27	7.30	42.8	18729.6	2.41	2031.40	25
27	Q66C1.66	3	66	1.66	18.45	21.6	23957.4	0.19	5319.73	20
28	Q32C2.07	3	32	2.07	8.78	27.1	14245.5	1.05	2507.73	23
29	Q50C1.05	3	50	1.05	13.81	13.7	11374.7	0.22	4032.65	22
30	Q84C1.38	3	84	1.38	23.46	18.0	25403.0	0.10	6804.70	25
31	Q55C6	3	55	6.00	15.17	78.5	71436.9	1.02	3960.78	15
32	Q64C5.14	3	64	5.14	17.66	67.2	71230.5	0.65	4706.61	15
33	Q95C2.86	3	95	2.86	26.45	37.4	59352.5	0.16	7428.06	17
34	Q139C1.55	3	139	1.55	38.65	20.3	46983.1	0.04	11170.01	15
35	Q76.2C1.84	2	76	1.84	31.75	24.1	30557.7	0.05	6078.84	15
36	Q175.2C0.98	2	175	0.98	73.00	12.8	37420.4	0.00	14235.19	14
37	Q73.2C1.54	2	73	1.54	30.50	20.1	24568.6	0.04	5877.31	15
38	Q154.8C2.86	2	155	2.86	64.50	37.4	96490.6	0.02	12075.96	16

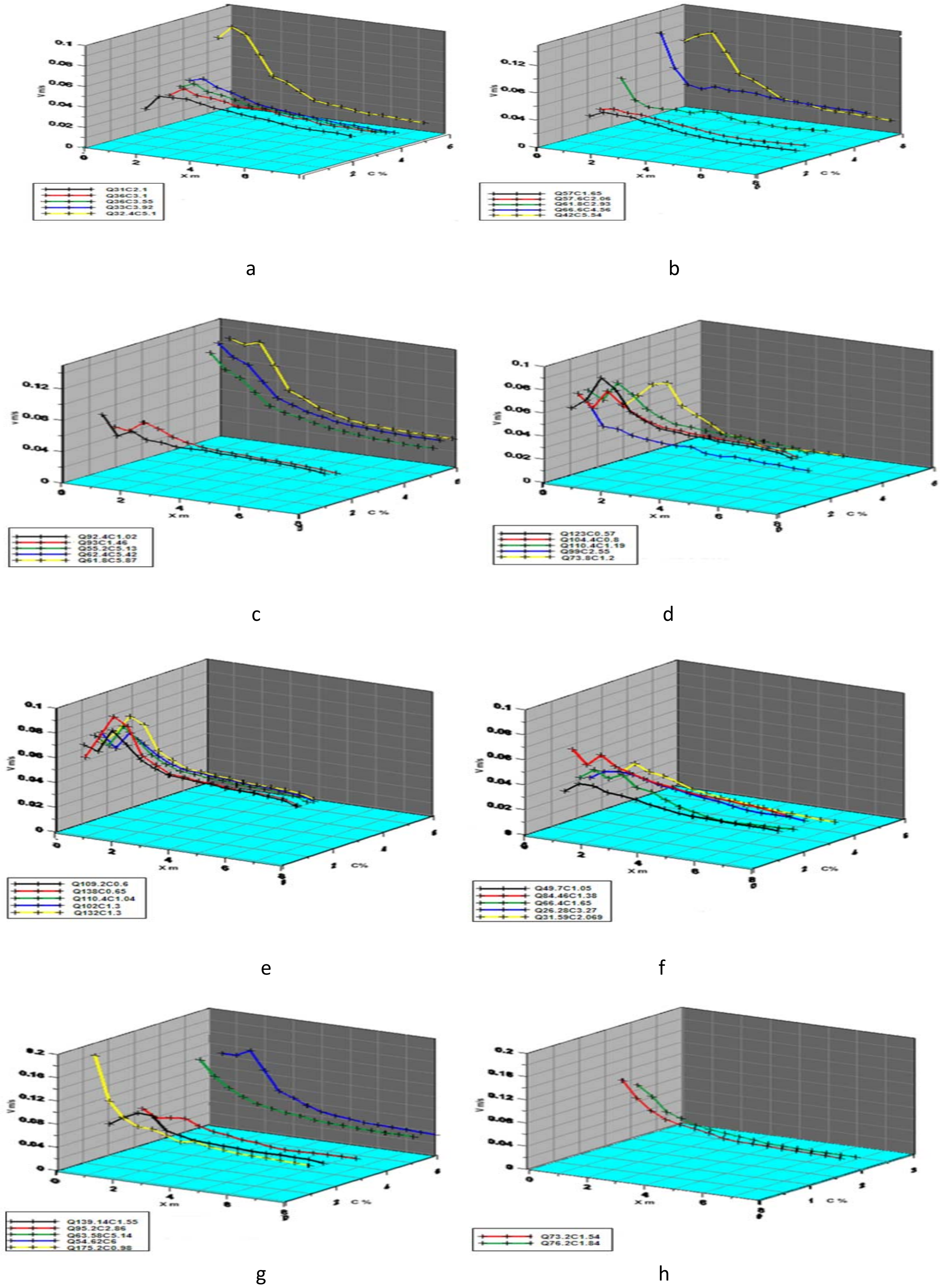

Fig 4. Changes in head velocity regarding various inflow concentration (C) and velocity (V)

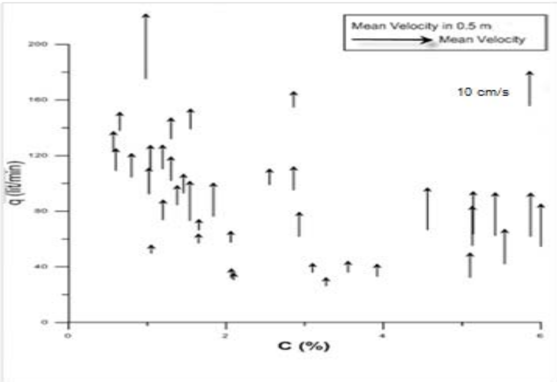
Mean Velocity in 0.5 m
Mean Velocity
10 cm/s
q (lit/min)
C (%)

I

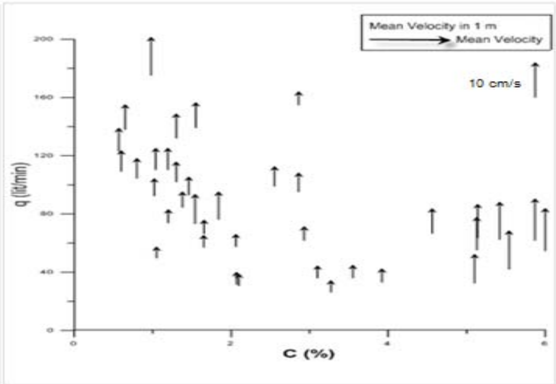
Mean Velocity in 1 m
Mean Velocity
10 cm/s
q (lit/min)
C (%)

h

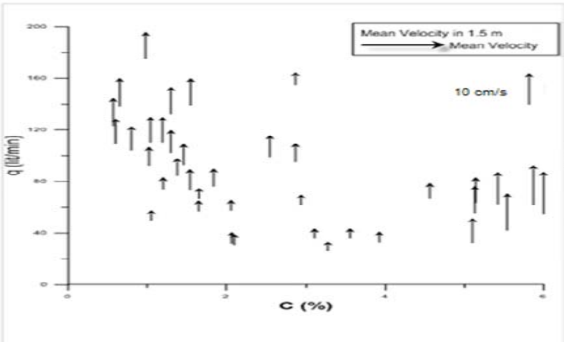
Mean Velocity in 1.5 m
Mean Velocity
10 cm/s
q (lit/min)
C (%)

I

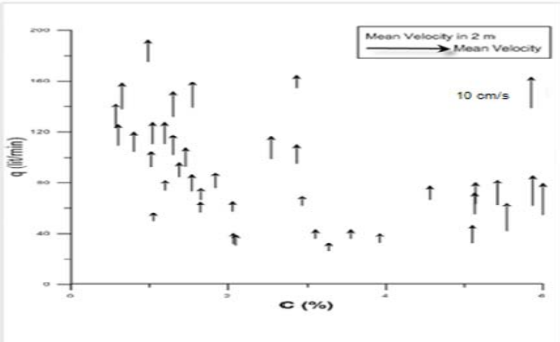
Mean Velocity in 2 m
Mean Velocity
10 cm/s
q (lit/min)
C (%)

j

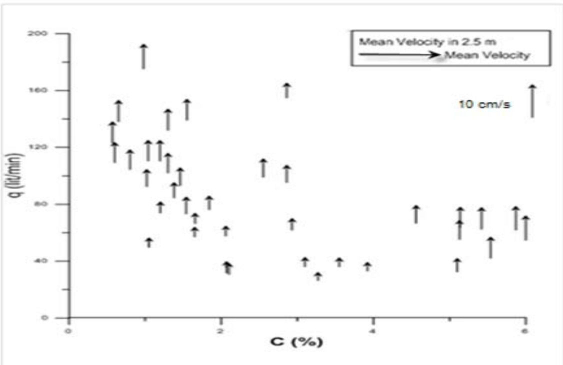
Mean Velocity in 2.5 m
Mean Velocity
10 cm/s
q (lit/min)
C (%)

k

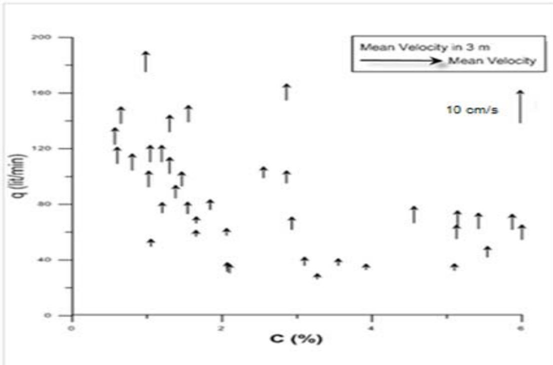
Mean Velocity in 3 m
Mean Velocity
10 cm/s
q (lit/min)
C (%)

l

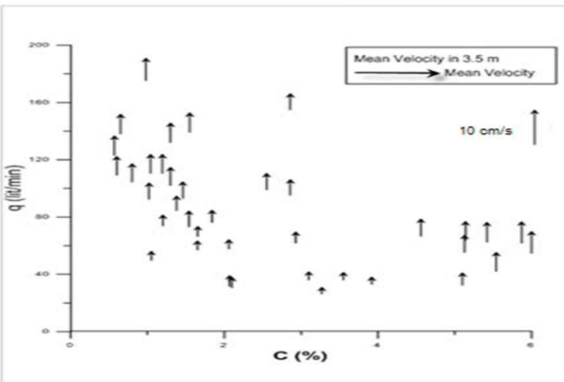
Mean Velocity in 3.5 m
Mean Velocity
10 cm/s
q (lit/min)
C (%)

m

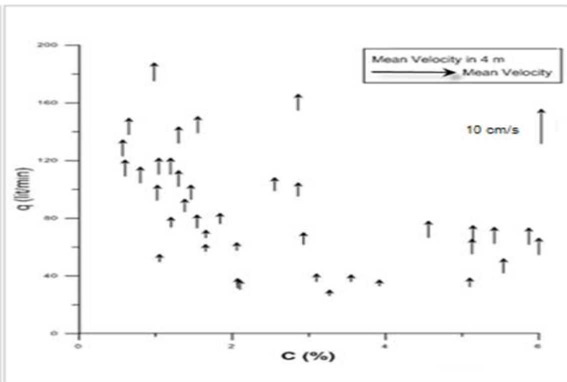
Mean Velocity in 4 m
Mean Velocity
10 cm/s
q (lit/min)
C (%)

n

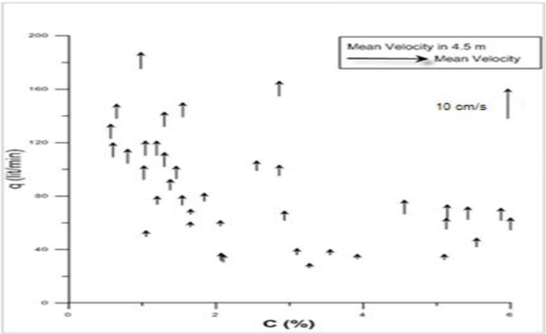

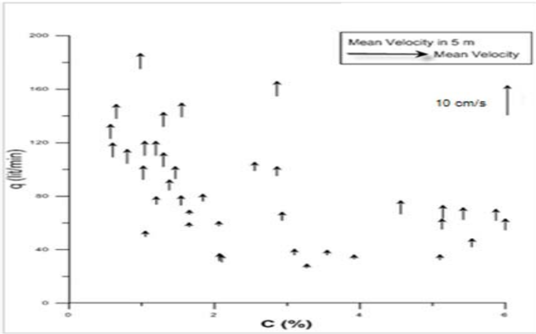

o p

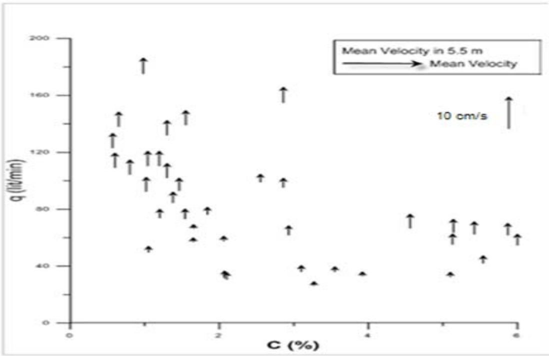

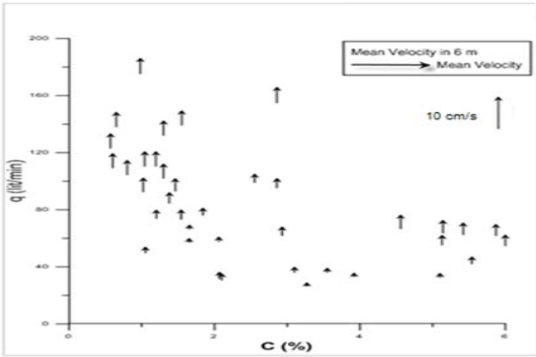

q r

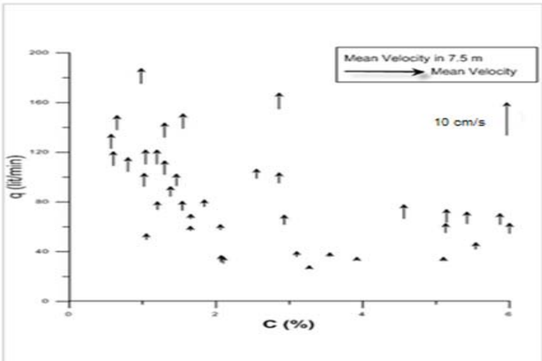

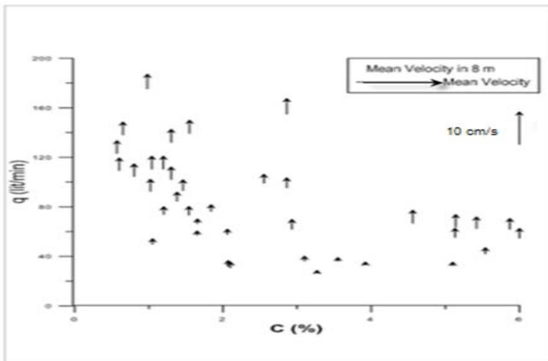

s t

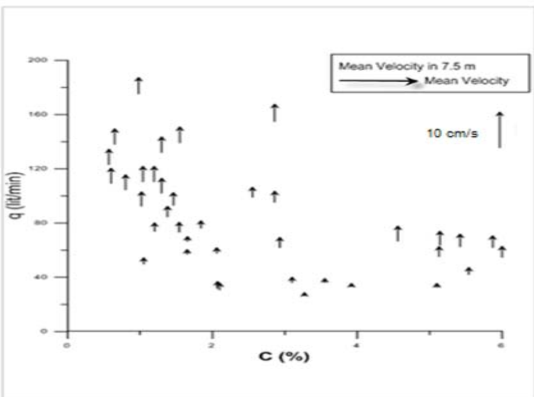

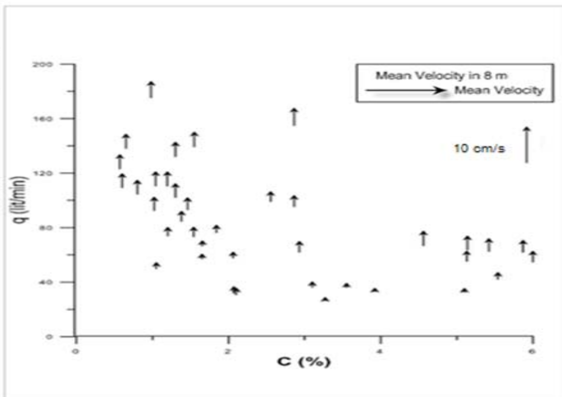

u v

Fig 5. Head velocity amount (cm/s) in each 0.5 meter section interval (0.5 to 8 m)

$$U_F = 1.6 \pm 0.3\sqrt[3]{g'q} \quad (11)$$

In most models, short length or width may causes some problems for direct observation while we survey the density currents lengthwise and crosswise motions. 38 tests were chose for studying the effects of different concentration and inflow discharge on the current head velocity. Lengthwise head velocity was estimated by recording time in each 0.5 meter lengthwise intervals. Lateral coincidence was also estimated in the terms of time and place. Specifications of each experiment have been summarized in Table 2. h_0 is the height of gate openness, C_0 is the inflow current concentration, U0 is the mean velocity of inflow density current, g'_0 is the reduced gravity of inflow current; B_0 is the flex, Ri_0 is the Richardson number , Fr_0 is the Froude number and Re_0 is the Reynolds number for the inflow current. The parameters mentioned above are calculated using the following equations

$$U_0 = \frac{Q_o}{h_0 \times b} \quad (12)$$

$$g'_0 = \frac{\rho_t - \rho}{\rho} g = RgC_0 \quad (13)$$

$$Ri_0 = \frac{g'_0 h_0 \cos\theta}{U_0^2} = \frac{1}{Fr_0^2} \quad (14)$$

$$\mathrm{Re}_0 = \frac{\rho_t U_0 h_0}{\mu_t} \quad (15)$$

$$B_0 = g'_0 b_0 h_0 U_0 \quad (16)$$

$$\mu_t = \mu(1 - 1.35C_0)^{-2.5} \quad (17)$$

ρ and μ are density and viscosity of water respectively, ρ_t and μ_t are density and viscosity of density current ,θ is the slope angle of flume bed slope and h0 and b are high and wide of the gate respectively. Experiments 1 to 7, 26, 28 and 31 were done in subcritical flow regime and other experiments were done in supercritical regime (Garcia, 1993). Head velocity is depicted versus inflow concentration and mean velocity (Fig 4). The inflow mean velocity of current typically varies between 7.3 and 38.7 cm/s. At high concentration runs the head velocity reduced more rapidly in the proximal area of our model. In most experiments head velocity increased then reduced slightly near the entrance gate (Alexander and Mulder, 2002). The maximum velocity of sedimentary current occurred between 1 to 1.5 meters away from the entrance gate in comparison with Kneller et al. 1999 experiment indicated that the maximum velocity of the vertical profile occurs at 80cm of the flume outset (Kneller et al., 1999). After that point, the velocity has a decline trend throughout the flume due to reduction of the current progress power as a result of gradual sedimentation of suspended particles. Head velocity of the density current at various sections is illustrated in figure 5. At the proximal area, the head velocity reduction for high concentration inflow runs (>4%), varied between 11 to 33 percent (averagely 23%) and the velocity varied quiet a lot But in the run with low concentration inflow (< 2%) head velocity declines varied between 61 to 84 percent (averagely 75%). Consequently the

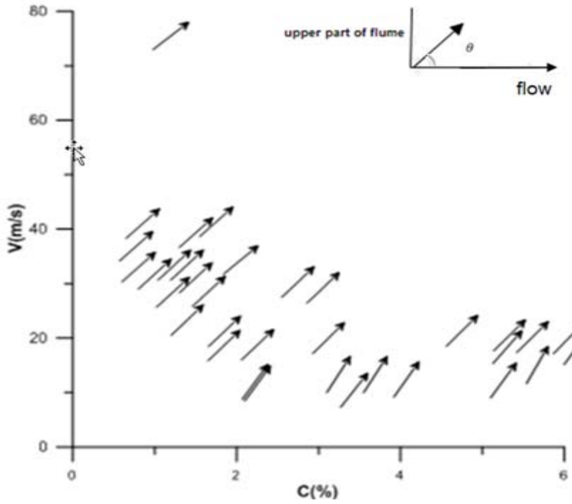

Fig 6. Deviation angle of lateral motion to the side

relative minimum decrease in the velocity of density current would be 2.38 percents and occurs at 1 meter away from the gate. According to the results illustrated to in Figure 5, an increase in the current's head velocity will be a function of concentration and inflow current velocity. Increasing the head velocity in low discharge runs could be observed when concentration is more than 4% and indeed an increase in velocity in low concentration runs could be observed at more than 80 lit/s inflow discharge (q = 0.4 m3/s/m).

Lateral motions of current to the sides

For most present models, short widths are considered. Therefore the lateral motions of currents are not attracted that much. In the model discussed in this article, regarding the 3 meters widths, the measurements of lateral motions have also been recorded in details. By taking in to consideration of different amounts of inflow concentration and velocity, the angle between current wave and flow direction has been plotted (Fig 6). The angle varies between 63 and 41 degrees and takes a higher amount for high concentration inflow runs Therefore it is expected that the particles are deposited near the upstream of flume. Also, a similar condition has been observed with regard to the fewer inflow velocity runs.

Conclusion

38 experiments were done in order to find out the effects of inflow current velocity and concentration on the head velocity of density current and the cross motion angle of current. It was observed that the maximum sedimentary current velocity in most of experiments occurs at a distance of 1 to 1.5 meters away from the entrance gate. Velocity during the flume length has a diminishing trend that is because of reduction in progression power of current and gradual deposition of suspended particles. In experiments with a high concentrated current (more than 4%), head velocity reduction in the first section (0.5 meter away from the entrance) varies between 11 and 33 percent (averagely 23%). Thus, at the runs with a low concentrated current (less than 2%), head velocity reduction varies between 61 and 84 percent (averagely 75%). By

increasing velocity or concentration, the side motion angle of current head that makes with the flow direction varies between 63 and 41 degrees and it takes a higher amount for high concentration runs, therefore, sedimentary particles deposit at closer distances away from the laboratory flume entrance.

References

Altinakar S, Graf WH, Hopfinger EJ (1990) Weakly depositing turbidity current on a small slope. J Hydraul Res 28:22-80

Alexander J, Mulder T (2002) Experimental quasi-steady density current. Mar Geol 186:195-210

Bagnold RA (1954) Experiments on gravity-free dispersion of large solid spheres in a Newtonian fluid under shear. Proc. Royal Soc. of London Ser A: 353

Barr DAH (1967) Densimetric exchange flow in rectangular channels, III, Large scale experiments. Houille Blanche 6: 619-631

Boillat J-L, De Cesare G (1994) Dichteströmungen im Bereich des Grundablasses des Stausees Luzzone – Modellversuche Proceedings of the Symposium. Betrieb Erhaltung und Erneuerung von Talsperren und Hochdruckanlagen, Graz, Austria, 183-192

Britter RE, Linden PF (1980) The Motion of the Front of a Gravity Current Traveling Down on an Incline. J Fluid Mech 99:531 -543

Buckee C, Kneller B, Peakall J (2001) Turbulence structure in steady, solute-driven gravity currents. In McCaffrey, W.D.,Kneller, B.C., Peakall, J. (eds). Particulate Gravity Currents, IAS Special Publication 31: 173-187

Chikita K (1990) Sedimentation by river-induced turbidity currents: field measurements and interpretations. Sedimentology 37:891-905

Chio SU, Garcia MH (1995) Modeling of one-dimensional turbidity current with a dissipative Galerkin finite element method. J Hydraul Res, 33(5):1-26

De Cesare G (1998) Alluvionnement des retenues par courants de turbidite'. PhD Thesis Nº 1820 and Communication du Laboratoire de constructions hydrauliques - LCH N° 7, Lausanne, EPFL, Switzerland

Ellison TH, Turner JS (1959) Turbulent entrainment in stratified flows. J Fluid Mech 6: 423-448

Fan J, Morris GL (1992) Reservoir Sedimentation II: Reservoir Desiltation and Long-term Storage Capacity. J Hydraul Eng 118(3): 370-384

Fukushima Y, Parker GA, Pantin HM (1985) Prediction of the ignitive turbidity currents in Scripps Submarine Canyon. Mar Geol 67:55-81

Garcia MH (1985) Experimental study of turbidity currents. M.Sc. thesis, Dept. of Civil and Mineral Engineering, University of Minnesota, USA.

Garcia MH (1993) Hydraulic jumps in sediment-driven bottom currents. J Hydraul Eng 119:1094-1117

Harleman DRF (1961) Stratified flow. Handbook of fluid dynamics. V Streester, ed. McGraw-Hill, New York

Hebbert B, Imberger J, Loh I, Patterson J (1979) Collie river underflow into the Wellington reservoir. J Hydraulics Div ASCE 105(5): 533–545

Hinze JO (1960) On the Hydrodynamics of Turbidity Currents. Geologie en Mijnbouw 39:18-25

Hoogendoorn RM (2006) The impact of changes in sediment supply and sea-level on fluvio-deltaic stratigraphy. Ph.D thesis Delft, Univ Technol, The Netherlands, p 159

Hopfinger EJ, Tochon-Danguy JC (1977) A model study of powder-snow avalanches. Journal of Glaciology 19(81): 343-356

Keulegan GH (1957) An experimental study of the motion of saline water from locks into fresh-water channels. US Natl Bur Stand, Report 5168

Keulegan GH (1958) The motion of saline fronts in still water. U.S. Nat. Bur. of St., Paper 5831

Kneller BC, Bennet SJ, McCaffrey WD (1997) Velocity and turbulence structure of gravity currents and internal solitary waves: potential sediment transport and the formation of wave ripples in deep water. Sedimentary Geology 112:235-250

Kneller BC, Bennet SJ, McCaffrey WD (1999) Velocity structure, turbulence and fluid stresses in experimental gravity currents. Journal of Geophysical Research 104(C3):5381-5391

Lee HY, Yu WS (1997) Experimental study of reservoir turbidity current. J Hydraul Eng ASCE 123(6):520–528

Lowe RJ, Linden PF, Rottman JW (2002) A laboratory study of the velocity structure in an intrusive gravity current. J Fluid Mech 456 :33-48

Mahmood K (1987) Reservoir Sedimentation – Impact, Extend and Mitigation. World Bank Technical Paper Number 71, Washington D.C.

Marino BM, Thomas LP, Linden PF (2005) The front condition for gravity currents. J. Fluid Mech 536:49–78

Middleton GV, (1966) Experiments on density and turbidity currents. I. Motion of the head. Can J Earth Sci 3: 523- 546

Moghtaderi B (2004) Application of laser Doppler velocimetry (LDV) to study the influence of heat transfer on the structure of gravity currents. Experimental Thermal and Fluid Science 28:843–852

Morris SA, Kenyon NH, Limonov AF, Alexander J, (1998) Downstream changes of large-scale bedforms in turbidites around the Valencia channel mouth, north-west Mediterranean: implications for palaeoflow reconstruction. Sedimentology 45:365-377

Mulder Th, Savoye B, Syvitski JPM, Parize O (1997) Des courants de turbidité hyperpycnaux dans la tête du canyon du Var? Observations hydrologiques et données de terrain. Oceanologica Acta 20(4): 607-626

Parker GA, Fukushima Y, Pantin HM (1986) Self-acceleration turbidity currents. J Fluid Mech. 171:145-181

Parsons JD, Garcia MH (1998) Similarity of gravity current fronts. Phys Fluids 10: 3209-3213

Parsons J D, Friedrichs CT, Trykovski P, Mohrig D, Imran J, Syvitski JPM, Parker G, Puig P, Garcia MH (2007) The mechanics of marine sediment gravity fows. Continental Margin Sedimentation: Transport to Sequence. IAS Special Publication 37, Blackwell Publishing Ltd, Oxford (C. Nittrouer Editor), p. 275-338.

Postma G, Nemec W, Kleinspehn KL (1988) Large floating clasts in Turbidites: a mechanism for their emplacement. Sedimentary Geology 58:47-61

Samothrakis P, Cotel AJ (2006) Propagation of a gravity current in a two-layer stratified environment. J Geophysical Res 111:1-17

Simpson JE (1987) Gravity Currents in the Environment and the Laboratory. Halsted, Chichester, p 244

Simpson JE (1997) Gravity currents in the environment and in the laboratory. 2nd edn. Cambridge University Press, Ellis-Hornwood, Chichester

Simpson JE, Britter RE (1979) The dynamics of the head of a gravity current advancing over a horizontal surface. J Fluid Mech. 94:477-495

Turner JS (1979) Bouyancy effects in fluids. Cambridge University Press

Yu W, Lee H, Hsu Sh M (2000) Experiments on deposition behavior of fine sediment in a reservoir. J Hydraul Eng ASCE 126 (12): 912-920